

# Influence of composition and molecular mass on the morphology, crystallization and melting behaviour of poly(ethylene oxide)/poly(methyl methacrylate) blends

E. Martuscelli\*, M. Pracella† and Wang Ping Yue‡

*Istituto di Ricerche su Tecnologia dei Polimeri e Reologia del CNR, Arco Felice (NA), Italy*

(Received 16 June 1983; revised 6 September 1983)

Results are reported on the influence of composition and molecular mass of components on the isothermal growth rate of spherulites, on the overall kinetic rate constant, on the primary nucleation and on the thermal behaviour of poly(ethylene oxide)/poly(methyl methacrylate) blends. The growth rate of PEO spherulites as well as the observed equilibrium melting temperatures decrease, for a given  $T_c$  or  $\Delta T$ , with the increase of PMMA content.

Such observations are interpreted by assuming that the polymers are compatible in the undercooled melt, at least in the range of crystallization temperatures investigated. Thermodynamic quantities such as the surface free energy of folding  $\sigma_e$  and the Flory-Huggins parameter  $\chi_{12}$  have been obtained by studying the dependence of the radial growth rate  $G$  and of the overall kinetic rate constant  $K$  from temperature and composition and the dependence of the equilibrium melting temperature depression  $\Delta T_m$  upon composition, respectively.

(Keywords: blends; poly(ethylene oxide); poly(methyl methacrylate), morphology; crystallization, melting)

## INTRODUCTION

In previous work, Martuscelli and coworkers<sup>1</sup> reported that blends of poly(ethylene oxide) (PEO) with molecular weight  $M_w=20\,000$  and poly(methyl methacrylate) (PMMA) with  $M_w=110\,000$  show, for contents of PMMA up to 40% by weight, a well defined spherulitic morphology, depression of spherulite growth rate and of observed melting temperature and a single glass transition, composition dependent, intermediate between those of the pure components. Such behaviour was interpreted by assuming that the two polymers are miscible at the molecular level in the molten state. Direct evidence of compatibility of PEO and PMMA in the melt was obtained by Martuscelli *et al.*<sup>2</sup> by investigating the <sup>13</sup>C n.m.r. behaviour of their blends at 90° and 60°C.

Moreover the compatibility between these two polymers was theoretically predicted also on the basis of both 'lattice' theory and the solubility parameter approach<sup>3</sup>.

In the present paper, the influence of composition on the isothermal growth rate of spherulites, on the overall kinetic rate constant, on the primary nucleation and on the thermal behaviour is studied in the case of PEO/PMMA blends with plain PEO and PMMA having molecular mass of 100 000 and 110 000 respectively. Some

of the results are compared with those previously obtained on blends containing PEO with  $M_w=20\,000$ .

The main goal of the work is to examine the influence of molecular mass of crystallizable component on some of the properties of the system. Further results are reported on some kinetic, morphological and nucleation aspects that in the first paper were not deeply investigated.

## EXPERIMENTAL

Blends of poly(ethylene oxide) (PEO10, Fluka AG product,  $M_w=100\,000$ ) and poly(methyl methacrylate) (PMMA, BDH product,  $M_w=110\,000$ ;  $M_v=116\,000$  from viscosity measurements in  $\text{CHCl}_3$  at 25°C) from 100% to 60% by weight of PEO were prepared by solution casting from  $\text{CHCl}_3$  and then drying under vacuum at 80°C for 24 h, to remove the residual solvent.

The morphology and the isothermal growth rate  $G$  of PEO spherulites in the blends were studied on thin films by using a Reichert polarizing optical microscope equipped with a Mettler calibrated hot stage (precision  $\pm 0.2^\circ\text{C}$ ). The films were first melted at 85°C for 5 min; after that they were rapidly cooled at a fixed crystallization temperature  $T_c$  and the radius of growing spherulites was measured as a function of time.

The overall crystallization kinetics from melt blends was analysed by differential scanning calorimetry with a Perkin-Elmer DSC-2 apparatus.

The samples (about 5 mg in weight) were heated, after melting, at 85°C for 5 min, then isothermally crystallized at various  $T_c$ , recording the heat of crystallization as a function of permanence time at  $T_c$ . The fraction of  $X_t$  of

\* To whom all correspondence should be addressed

† Present address: Centro Studi Processi di Polimerizzazione e Proprietà Fisiche e Tecnologiche dei Sistemi Macromolecolari del CNR, Pisa, Italy

‡ Present address: North Western Chemical Power Corp., Xian, China

material crystallized after time  $t$  was determined by means of the relation:

$$X_t = \frac{\int_0^t \left(\frac{dH}{dt}\right) dt}{\int_0^\infty \left(\frac{dH}{dt}\right) dt}$$

where the first integral is the heat generated at time  $t$  and the second is the total heat of crystallization for  $t = \infty$ .

The observed melting temperatures  $T_m'$  of the isothermally crystallized blends were measured both by d.s.c. and optical microscopy by heating the samples from  $T_c$  up to  $T_m'$  with heating rates of  $20^\circ\text{C min}^{-1}$  and  $1^\circ\text{C min}^{-1}$  respectively. The mass crystallinity index  $X_c$  of the blends and of the PEO phase was calculated at various  $T_c$  from the ratios between the apparent enthalpies of fusion  $\Delta H^*$  and the enthalpy of fusion  $\Delta H$  of 100% crystalline PEO.

## RESULTS AND DISCUSSION

### *Morphology and spherulite growth rate*

Thin films of PEO10/PMMA blends isothermally crystallized in the temperature range  $39^\circ\text{--}56^\circ\text{C}$  (312–329 K) show for all the compositions examined the characteristic spherulite morphology of melt crystallized PEO. At the optical microscope, under crossed Nicols, the

spherulites display a 'Maltese cross' birefringent pattern and have regular shape with defined borders: no separated domains of uncrystallizable PMMA component are observed in the intra-spherulitic regions nor in the inter-spherulitic contact zones. Moreover after crystallization the PEO/PMMA films appear completely filled with impinged spherulites.

Figure 1 shows optical micrographs of spherulites crystallized from melt PEO10/PMMA blends with different composition. Spherulites of 60/40 blend show a less regular texture; this may be referred to the coarseness of the crystalline lamellae due to the presence of uncrystallized material in interlamellar regions. With de-

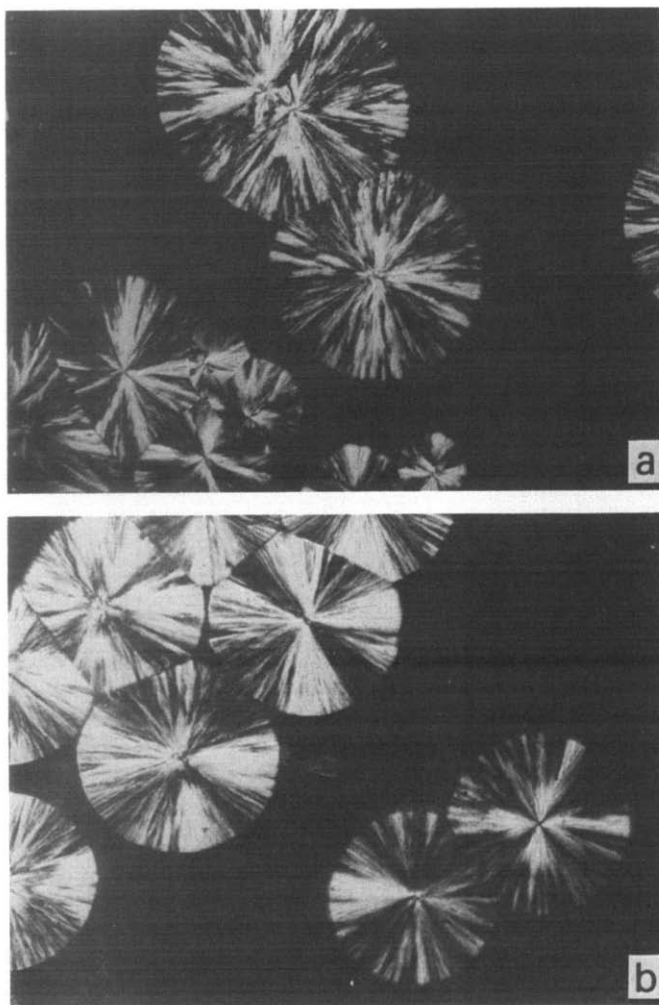
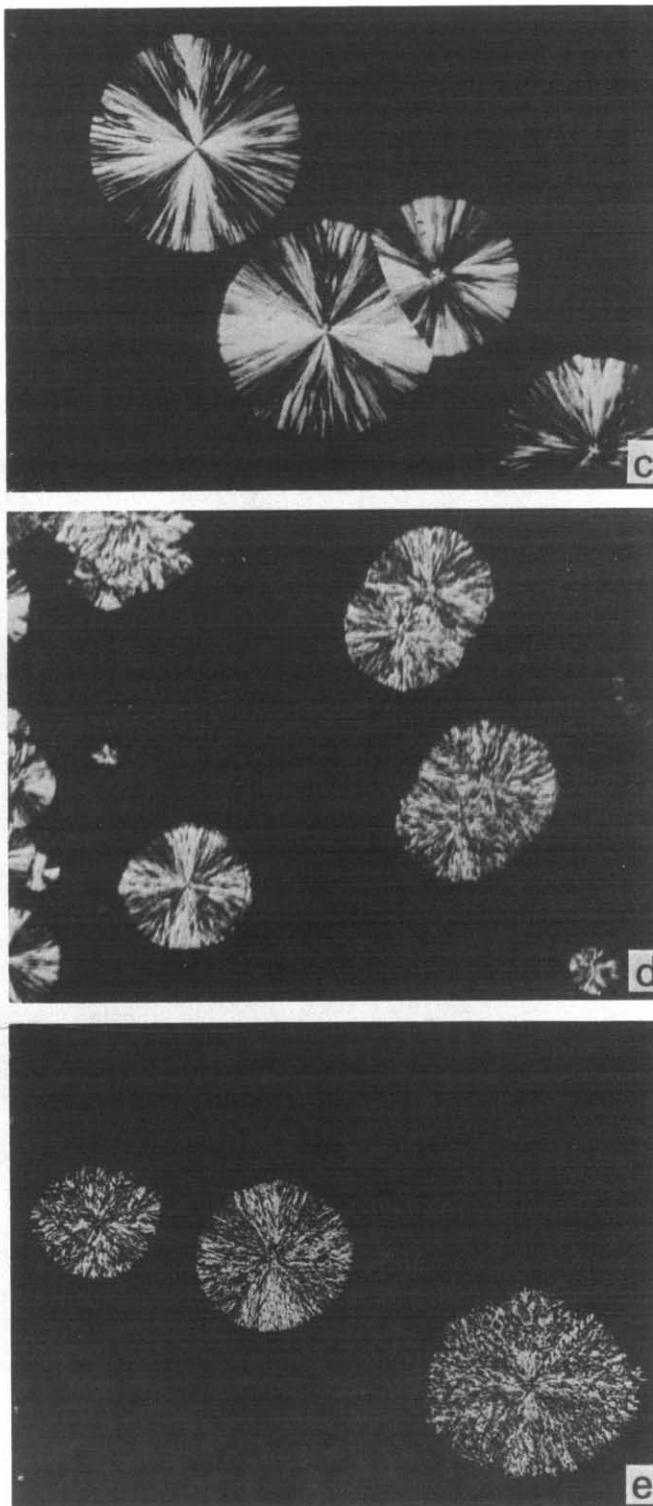


**Figure 1** Optical micrographs (crossed polars) of spherulites growing in thin films of PEO and PEO/PMMA blends of various composition: (a) PEO10,  $T_c=49^\circ\text{C}$  (46.4x); (b) PEO/PMMA (90/10),  $T_c=48^\circ\text{C}$  (60.7x); (c) PEO/PMMA (80/20),  $T_c=48^\circ\text{C}$  (50.8x); (d) PEO/PMMA (70/30),  $T_c=48^\circ\text{C}$  (72.8x); (e) PEO/PMMA (60/40),  $T_c=46^\circ\text{C}$  (50.8x)



creasing crystallization temperature  $T_c$ , the effect of uncrystallized material deteriorating the texture of the spherulites becomes more pronounced.

Moreover for blends of PEO  $M_w = 20\,000$  (PEO2) with PMMA it has been reported that the spacing, measured by small-angle X-ray scattering, increases with  $T_c$  and PMMA concentration<sup>4</sup>.

All these observations suggest that during the crystallizing process of the blends, the PMMA is incorporated in the interlamellar regions of PEO spherulites.

A similar behaviour has also been found in the case of other compatible blends such as poly(caprolactone)/poly(vinyl chloride)<sup>5</sup> and poly(vinylidene fluoride)/PMMA. For those systems too the non-crystallizable component has a higher glass transition temperature.

The spherulite radius  $R$  increases linearly with time for all the temperatures and blend compositions investigated. Variations of the slope  $dR/dt$  were not observed over long crystallization times, indicating that during the growth

the concentration of PMMA at the tips of radial lamellae does not change. The values of spherulite growth rate  $G$  of plain PEO10 and of PEO crystallized from PEO10/PMMA blends are reported as a function of  $T_c$  in Table 1. The dependence of  $G$  on  $T_c$  is shown in Figure 2. It can be observed that, at a given  $T_c$ ,  $G$  decreases with increasing PMMA content. This effect of depression is much larger as the crystallization temperatures become lower. A depression of the spherulite growth rate of the crystallizable component has also been found in the case of poly(caprolactone)/poly(vinyl chloride) blends<sup>5</sup> and poly(vinylidene fluoride)/PMMA blends<sup>6</sup>.

The values of  $G$  of plain PEO2, PEO10 and of their corresponding blends with PMMA are compared at two different  $T_c$  (49° and 51°C) in Table 2. As shown,  $G$  of PEO2 and PEO2/PMMA blends is systematically higher than that of PEO10 and PEO10/PMMA blends respectively. However, it is interesting to underline that the percentage depression is almost independent of PEO molecular mass.

**Table 1** Values of the spherulite growth rate  $G$ , of the time of half-crystallization  $t_{0.5}$ , of the overall kinetic rate constant  $K_n$ , of the Avrami index  $n$  and of the observed melting temperature  $T_m'$ , at various crystallization temperatures  $T_c$ , for plain PEO10 and PEO10/PMMA blends

	$T_c$ (K)	$T_m'$ (K)	$t_{0.5}$ (min)	$K_n$ (min <sup>-n</sup> )	$n$	$G$ ( $\mu\text{m min}^{-1}$ )
Plain PEO10	327	341.8	42.9	$3.52 \times 10^{-5}$	2.63	
	326	341.0	21.3	$2.01 \times 10^{-4}$	2.66	10
	325	340.8	9.1	$1.48 \times 10^{-3}$	2.78	
	324	340.4	5.8	$5.18 \times 10^{-3}$	2.78	29
	323	340.3	3.1	$2.90 \times 10^{-2}$	2.77	68
	322	339.7	1.8	$1.40 \times 10^{-1}$	2.60	96
	321	339.6	2.0	$1.33 \times 10^{-1}$	2.31	153
	320	339.2	0.8	1.09	2.53	
PEO10/PMMA (90/10)	326	341.6	33.3	$8.46 \times 10^{-5}$	2.57	4
	325	341.2	16.6	$5.45 \times 10^{-4}$	2.54	7
	324	340.4	11.9	$1.20 \times 10^{-3}$	2.56	13
	323	339.9	5.4	$7.53 \times 10^{-3}$	2.67	16.5
	322	339.5	4.3	$1.43 \times 10^{-2}$	2.64	21.4
	321	339.3	3.1	$3.57 \times 10^{-2}$	2.60	32.8
	320	339.0	2.0	$1.14 \times 10^{-1}$	2.57	40
	319	338.7	1.4	$2.84 \times 10^{-1}$	2.52	
PEO10/PMMA (80/20)	323	340.7	39.1	$5.40 \times 10^{-5}$	2.50	
	322	340.5	33.1	$1.36 \times 10^{-4}$	2.44	8
	321	339.2	29.2	$1.00 \times 10^{-4}$	2.52	15
	320	338.8	19.0	$4.94 \times 10^{-4}$	2.46	18
	319	338.6	12.4	$7.01 \times 10^{-4}$	2.74	20
	318	338.3	10.1	$2.00 \times 10^{-3}$	2.52	26
	316	337.8	3.2	$3.95 \times 10^{-2}$	2.46	44
	315	337.5	3.4	$3.57 \times 10^{-2}$	2.45	
PEO10/PMMA (70/30)	322	339.1	72.4	$6.05 \times 10^{-6}$	2.72	3.8
	321	339.4	38.2	$2.48 \times 10^{-5}$	2.95	6.1
	320	338.1	33.2	$2.25 \times 10^{-5}$	2.95	6.1
	319	338.0	24.5	$6.49 \times 10^{-5}$	2.90	8.4
	318	337.6	21.8	$9.00 \times 10^{-5}$	2.90	9.8
	317	337.0	16.8	$2.90 \times 10^{-4}$	2.82	11.4
	316	336.8	17.4	$2.83 \times 10^{-4}$	2.73	15.0
	315	336.9	11.4	$7.63 \times 10^{-4}$	2.79	16.0
	314	336.5	9.4	$1.47 \times 10^{-3}$	2.74	18.3
	313	336.0	7.2	$3.00 \times 10^{-3}$	2.74	
	312	335.9	5.7	$9.26 \times 10^{-3}$	2.56	
	PEO10/PMMA (60/40)	320	339.1	79.6	$6.81 \times 10^{-7}$	3.16
319		337.9	65.1	$8.49 \times 10^{-7}$	3.26	2.6
318		337.6	53.7	$3.66 \times 10^{-7}$	3.04	3.4
317		337.3	42.7	$5.90 \times 10^{-6}$	3.11	4.8
316		337.0	34.7	$1.04 \times 10^{-5}$	3.13	5.9
315		336.8	32.2	$1.63 \times 10^{-5}$	3.07	
314		336.6	25.7	$2.65 \times 10^{-5}$	3.13	6.1
313		336.4	22.8	$3.09 \times 10^{-5}$	3.20	
312		336.0	19.0	$1.24 \times 10^{-4}$	2.93	7.5
311		336.0	17.0	$4.06 \times 10^{-4}$	2.62	

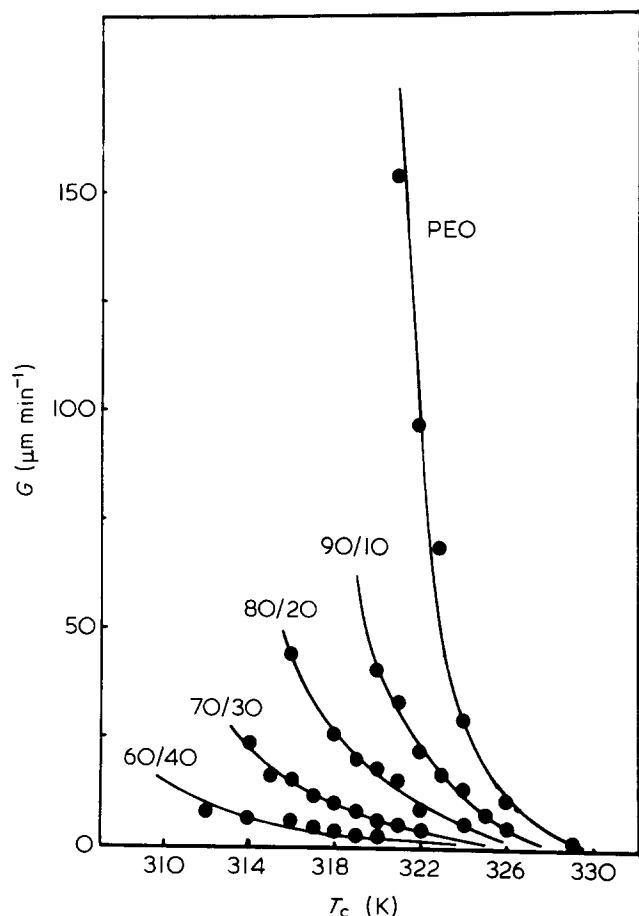


Figure 2 Radial growth rate  $G$  of spherulites in pure PEO and PEO/PMMA blends as a function of crystallization temperature

Table 2 Comparison between the  $G$  ( $\mu\text{m min}^{-1}$ ) of PEO2, PEO10 and their blends with PMMA

$T_c$ ( $^{\circ}\text{C}$ )		PEO (100%)	PEO/PMMA (80/20)		PEO/PMMA (70/30)	
		$G$	$G$	$\Delta$ (%)	$G$	$\Delta$ (%)
49	PEO2	324.8	28.3	91	10.0	97
	PEO10	96	8	92	3.8	96
51	PEO2	152.2	19.1	87	8.0	95
	PEO10	29	5	83	2	93

Overall rates of crystallization

By comparing, at the same  $T_c$ , the trends of the isotherms of crystallization of PEO10 and blends one observes that, on increasing the amount of PMMA in the samples, the overall crystallization rate becomes progressively slower and the isotherms are shifted along the time axis (see Figure 3).

The half-crystallization time  $t_{0.5}$ , defined as the time taken for half of the crystallinity to develop, is plotted against  $T_c$  for different blend compositions in Figure 4. The trends of such plots indicate that, at constant  $T_c$ , the overall crystallization rate of the blends decreases with increasing concentration of non-crystallizable component (for  $T_c = 320\text{ K}$  the  $t_{0.5}$  of the 70/30 blend is about forty times larger than that of pure PEO).

The kinetics of the isothermal crystallization from the melt of all PEO10/PMMA blends have been analysed on the basis of the Avrami equation:

$$X_t = 1 - \exp(-K_n t^n) \quad (1)$$

where  $K_n$  is the overall kinetic rate constant ( $K_n = \ln 2/t_{0.5}^n$ ) and  $n$  is a parameter that depends on the type of nucleation and on the geometry of growing crystals. Values for  $K_n$  and  $n$  have been derived, for each  $T_c$ , from the intercept and the slope of straight lines obtained by plotting the quantity  $\log[-\ln(1 - X_t)]$  against  $\log t$ .

Examples of such plots are shown in Figure 5a and b for 80/20 and 60/40 PEO10/PMMA blends. The observed linear trends indicate that for all the temperatures investigated the crystallization kinetics of these blends follow the Avrami equation until a high degree of conversion. The values of  $k_n$ ,  $n$  and  $t_{0.5}$  are reported in

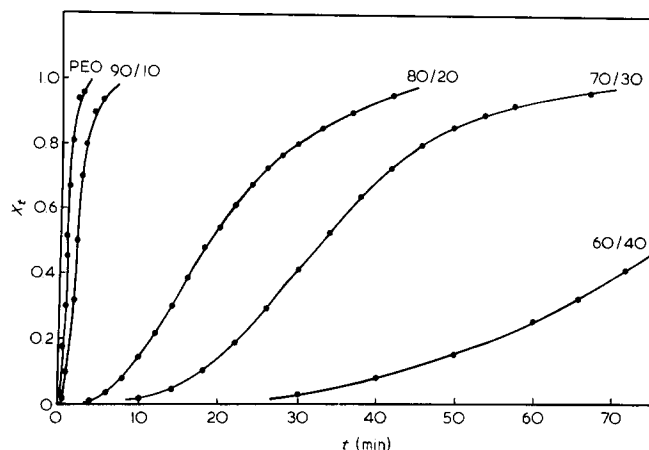


Figure 3 Influence of blend composition on the trend of the isotherms of crystallization ( $T_c = 320\text{ K}$ )

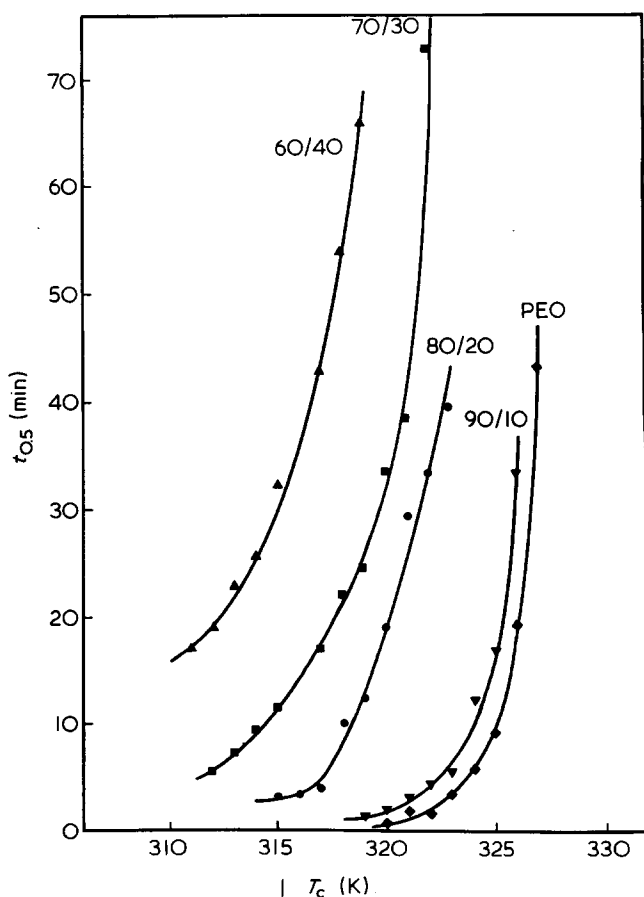


Figure 4 Half-time of crystallization  $t_{0.5}$  versus  $T_c$  for PEO10 and PEO10/PMMA blends

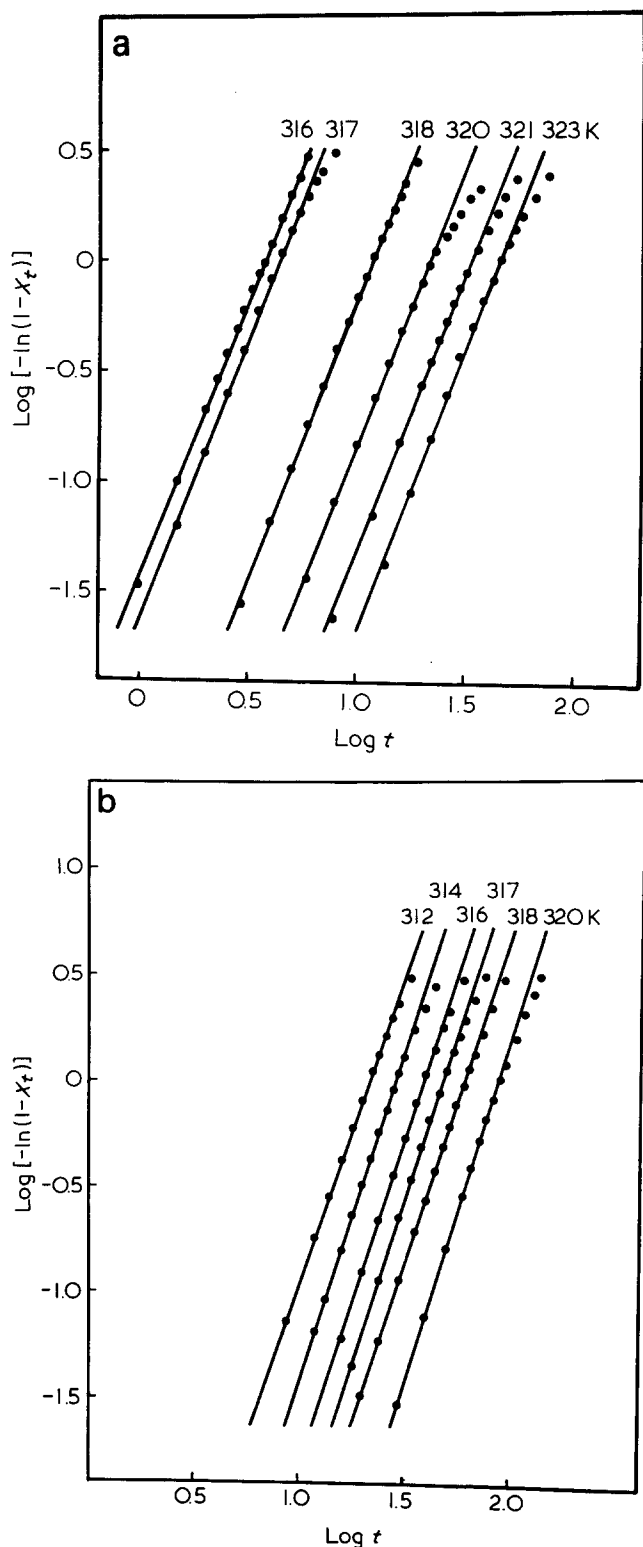


Figure 5 Avrami plots for: (a) PEO10/PMMA (80/20) blend; (b) PEO10/PMMA (60/40) blend

Table 1 for each of the blends investigated, as functions of  $T_c$ .

The mean values of the Avrami index  $n$  of each blend range from 2.5 (for PEO/PMMA 80/20) to 3.1 (for PEO/PMMA 60/40); pure PEO10 has a value of  $n$  of about 2.6. This corresponds to a three-dimensional growth of 'crystalline units' according to a crystallization process developed by heterogeneous nucleation<sup>17</sup>.

As shown in Figure 6, plots of  $\log K_n$  versus  $T_c$  give straight lines with values of slopes that decrease with

increasing PMMA content. Further a strong depression effect on  $K_n$  following the addition of PMMA to PEO10 may be observed.

The number of primary nuclei per unit volume  $\bar{N}$  was obtained by means of the relation:

$$K_n = \frac{4}{3}\pi \frac{\rho_c}{\rho_a} \frac{G^3 \bar{N}}{[1 - \lambda(\infty)]} \quad (2)$$

which assumes spherical growth with instantaneous nucleation<sup>7</sup>. In equation (2)  $G$  and  $K_n$  are measured at the same  $T_c$ ;  $\rho_c$  and  $\rho_a$  are the densities of the crystalline and amorphous phases respectively and  $1 - \lambda(\infty)$  is the crystalline weight fraction at time  $t = \infty$ .

For calculating  $\bar{N}$  it has been assumed that PEO and PMMA are miscible in the amorphous phase in all the composition range examined. Thus  $\rho_a$  and  $1 - \lambda(\infty)$  represent the density and the crystallinity of the blends respectively. The values of density  $\rho_a$  therefore have been calculated according to the relation:

$$\rho_a = 1/V_a = 1/(W_{\text{PEO}}V_{\text{PEO}} + W_{\text{PMMA}}V_{\text{PMMA}})$$

where  $W$  and  $V$  are the weight and specific volumes of the two components. It is found that, for a given composition, the number of nuclei decreases with increasing temperature but for a given  $T_c$  it does not vary regularly with the blend composition.

A decrease of the number of nuclei per unit volume with decreasing  $T_c$  and, for the same  $T_c$ , with increasing fraction of uncrystallizable component was found in the case of PCL/PVC blends<sup>5</sup>.

#### Melting and thermal behaviour

As shown by Figure 7 the observed melting temperature  $T_m$  of PEO10 and PEO10/PMMA blends increases li-

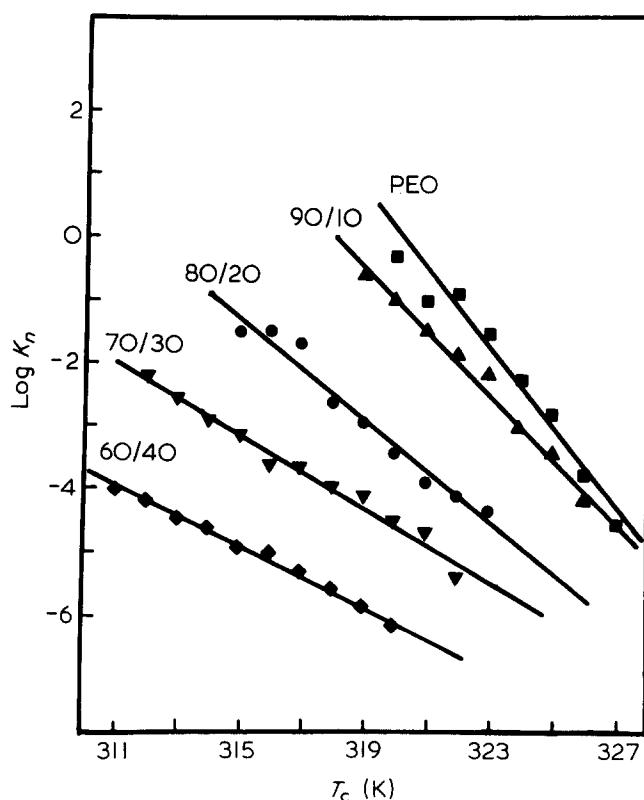


Figure 6 Variation of  $\log k_n$  with  $T_c$  for PEO10 and PEO10/PMMA blends

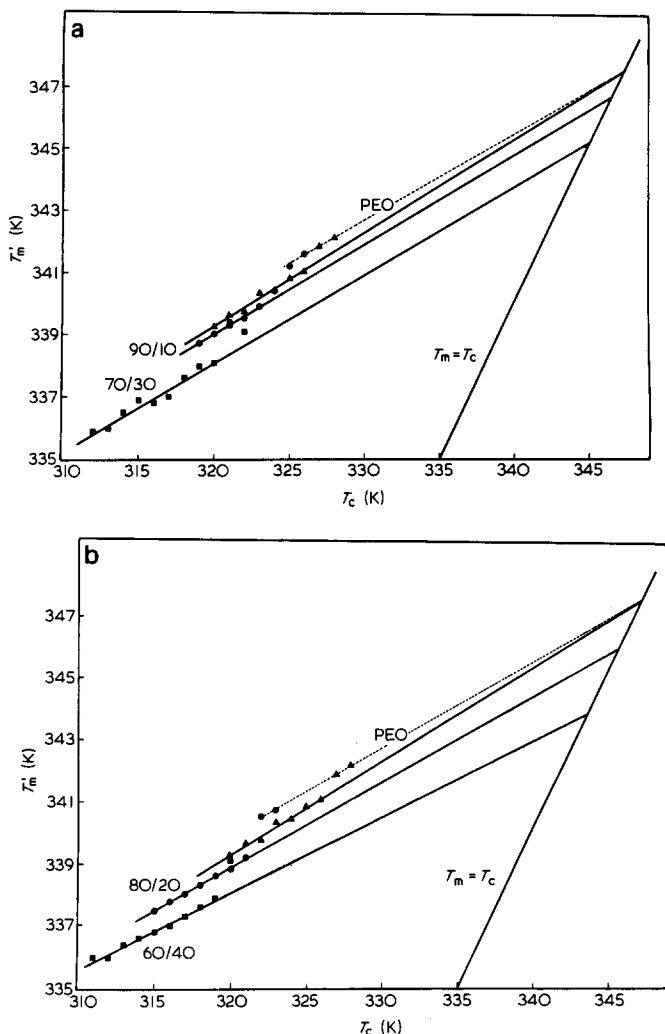


Figure 7 Plots of the observed melting temperature  $T_m$  versus  $T_c$  for PEO10 and PEO10/PMMA blends: (a) PEO10, PEO10/PMMA (90/10) and PEO10/PMMA (70/30); (b) PEO10, PEO10/PMMA (80/20) and PEO10/PMMA (60/40)

nearly with the crystallization temperature for a wide range of undercooling. A depression of  $T'_m$  for the same  $T_c$ , is observed for blends. The magnitude of this effect increases with increase of PMMA content.

At very high  $T_c$ , i.e. at low undercoolings, the observed melting points of blends undergo an abrupt increase and approach the values of  $T'_m$  of pure PEO. For  $T_c$  higher than  $53^\circ\text{C}$  the PEO sample also shows higher melting temperatures which do not align with those corresponding to higher undercooling. This effect is probably of morphological and kinetic nature, as will be discussed later.

For blends containing PEO with  $M_w = 20\,000$  it was found by Martuscelli *et al.*<sup>1</sup> that  $T'_m$  increases linearly with  $T_c$  only at high undercooling. In fact at a well defined  $T_c$  an abrupt change in the slope was observed. The trend becomes non-linear and the melting point depression tends to vanish at low undercooling. The experimental data of the linear regions may be fitted by the equation:

$$T'_m = (1/\gamma)T_c + (1 - 1/\gamma)T_m \quad (3)$$

where  $T_m$  is the equilibrium melting temperature (Table 3) and  $1/\gamma$  is a morphological factor<sup>8</sup>. As shown in Figure 7 the lines  $T'_m - T_c$  extrapolate to values of  $T_m$  that are lower the higher the content of PMMA. The values of the slopes  $1/\gamma$  of the lines are almost independent of composition.

The finding that the morphological and stability parameter  $1/\gamma$  is almost constant and independent of blend composition and that the lines  $T'_m - T_c$  extrapolate to different equilibrium melting points strongly suggests that the melting point depression is primarily ascribed to the diluent effect of the non-crystallizable polymer as the two components are compatible in the melt.

The observation that at low undercooling the observed melting temperature depression tends to vanish may be accounted for by phase separation processes at  $T_c$  and/or partial melting and recrystallization phenomena during the heating up of the samples.

In Figure 8 the values of  $T_m$  or PEO10/PMMA blends are reported as a function of the composition. The upper line refers to the values determined by d.s.c. with heating rates of  $20^\circ\text{C min}^{-1}$ ; the lower line refers to optical microscopy measurements made with heating rate of  $1^\circ\text{C min}^{-1}$ . In both cases the equilibrium melting temperature exhibits a linear dependence from the blend composition according to a general expression:

$$T_m = T_m^0 - \alpha W_1$$

Table 3 Equilibrium melting temperature for plain PEO10 and for PEO10 crystallized from its blends with PMMA

Sample	Equilibrium melting temperature (K)
PEO10 (100%)	348
PEO10/PMMA (90/10)	347
PEO10/PMMA (80/20)	346
PEO10/PMMA (70/30)	345
PEO10/PMMA (60/40)	344

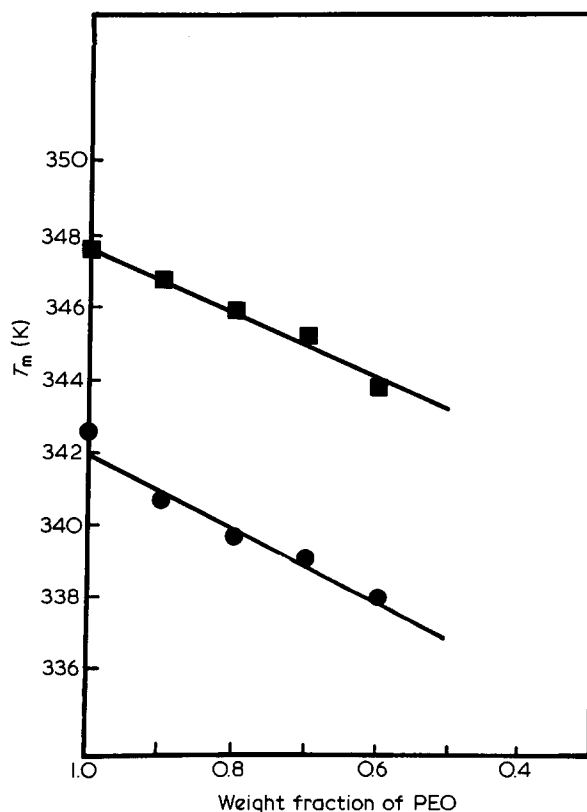


Figure 8 Equilibrium melting temperature  $T_m$  of PEO10/PMMA blends as a function of composition: upper line,  $T_m$  from d.s.c.; lower line,  $T_m$  from optical microscopy

where  $W_1$  is the weight fraction of PMMA in the blends,  $T_m^\circ$  is the equilibrium melting temperature of pure PEO and  $\alpha$  is about 8.5 K.

Such an expression is analogous to that derived by Sanchez and Eby<sup>9</sup> describing the depression of the equilibrium melting temperature of copolymer with varying concentration of non-crystallizing comonomer units.

The physical meaning of this parallelism is that for a compatible blend of two polymers, of which one is non-crystallizable, the melting behaviour behaves as a copolymer in which the units of the non-crystallizing component are statistically distributed along the macromolecule.

Following the thermodynamic treatment elaborated by Scott<sup>10</sup>, a quantitative analysis of the melting point depression has been presented by Nishi and Wang<sup>11</sup> and later by Imken *et al.*<sup>12</sup>

The results of this analysis lead to the conclusion that a plot of the melting point depression  $\Delta T_m = T_m^\circ - T_m$  versus the square of the volume fraction of non-crystallizable component  $v_1^2$  should be linear with an intercept at the origin if there are no entropic contributions to  $\Delta T_m$ , according to the relation:

$$\Delta T_m = -T_m^\circ [V_{2\mu}/\Delta H_{2\mu}] B v_1^2 \quad (5)$$

with

$$B = RT\chi_{12}/V_{1\mu}$$

In equation (5) the ratio  $\Delta H_{2\mu}/V_{2\mu}$  gives the latent heat of fusion of 100% crystalline component per unit volume;  $V_{1\mu}$  is the molar volume of non-crystallizable component and  $\chi_{12}$  is the Flory-Huggins interaction parameter.

As shown in Figure 9 the melting point depression  $\Delta T_m$  of PEO/PMMA increases linearly with  $v_1^2$  according to the following equation:

$$\Delta T_m = 20.15 v_1^2 + 0.7 \quad (6)$$

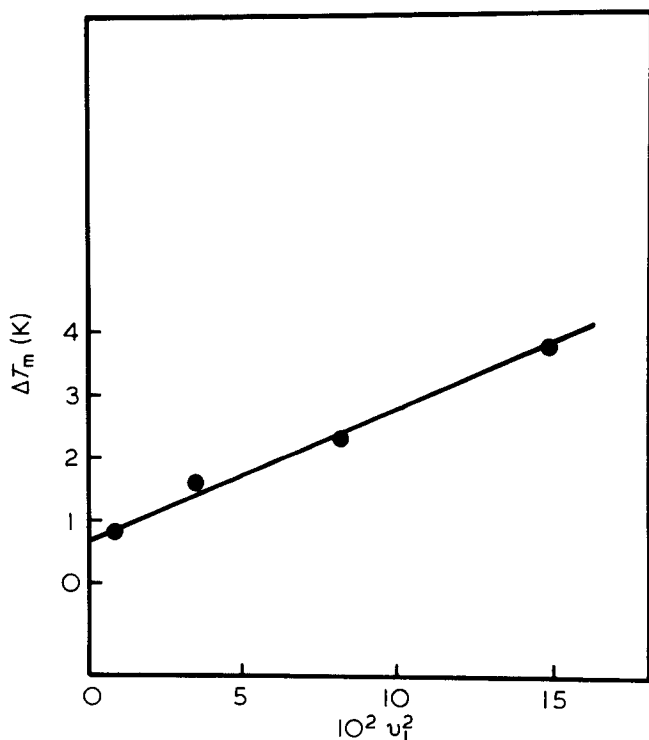


Figure 9 Variation of the equilibrium melting temperature depression  $\Delta T_m$  with the square of the volume fraction of PMMA,  $v_1^2$ .

Table 4 Values of the interaction energy density  $B$  and of the interaction parameter  $\chi_{12}$  for binary blends with components compatible in the melt

System	$B$ (cal cm <sup>-3</sup> )	$\chi_{12}$	Ref.
PVF <sub>2</sub> /PEMA (Imken <i>et al.</i> ) (Kwei <i>et al.</i> )	- 3.18 - 2.86	-0.34 (at 160°C)	12
PVF <sub>2</sub> /PMMA (Nishi <i>et al.</i> )	- 2.98	-0.295 (at 160°C)	11
PEO(20 000)/PMMA (Martuscelli and Demma)	-15.6	-1.93 (at 76°C)	1
PEO(100 000)/PMMA (Present work)	- 2.85	-0.35 (at 74°C)	

Published density data<sup>13</sup> were used to convert weight fraction into volume fractions. By using equation (5) from the slope of the line of Figure 9 we deduced for  $B$  a value of  $-2.85$  cal cm<sup>-3</sup> from which a value of  $-0.35$  was calculated for  $\chi_{12}$  at the equilibrium melting temperature of plain PEO (74°C). For  $V_{1\mu}$ ,  $V_{2\mu}$  and  $\Delta H_{2\mu}$  the following values were used respectively: 40.32 cm<sup>3</sup> mol<sup>-1</sup>, 85.87 cm<sup>3</sup> mol<sup>-1</sup> and 1980 cal mol<sup>-1</sup>. As reported in Table 4, these values are very close to those reported for other compatible polymer blends like poly(vinylidene fluoride)/poly(ethyl methacrylate) and poly(vinylidene fluoride)/poly(methyl methacrylate).

The negative values found for  $\chi_{12}$  in the case of PEO/PMMA blends supports the idea that this system is compatible in the melt and the fact that the intercept of equation (5) is close to zero indicates that entropic effects contribute little to  $\chi_{12}$ . Even in the case of blends with PEO of  $M_w = 20\,000$ , a plot of  $\Delta T_m$  versus  $v_1^2$  is linear but the intercept is far from zero and the absolute value of  $\chi_{12}$  that results is too large in comparison with literature data on compatible blends. The observations suggest for such blends:

- (i) non-negligible entropic effects occur during mixing of the two polymers;
- (ii) non-compliance with the assumption inherent in the extrapolation of  $T_m$  by using the Hoffman-Weeks plots;
- (iii) the inadequacies of the Flory-Huggins theory to describe the melting behaviour of such polymer-polymer systems.

The crystallinity index values of the blends ( $X_c(\text{blend})$ ) and of PEO ( $X_c(\text{PEO})$ ) are reported in Table 5 for each composition and  $T_c$  explored. From the data it can be observed that for a given composition  $X_c(\text{blend})$  is only slightly influenced by  $T_c$  while at constant  $T_c$  it decreases, as expected, with increasing PMMA concentration, going from a value of about 0.8 for pure PEO to a value of about 0.4 for the (60/40) PEO/PMMA blend.

As far as the crystallinity index of the PEO phase is concerned it emerges that  $X_c(\text{PEO})$ , at a given undercooling ( $\Delta T$ ), decreases with increase of PMMA content while for a fixed composition it decreases with increasing  $\Delta T$ . This trend may be accounted for by assuming that the relative amount of PMMA trapped in interlamellar regions of PEO spherulites increases with increase of the crystallization rate (that is, at higher values of  $\Delta T$ ) and with the starting PMMA concentration in the blend. As a consequence, at larger  $\Delta T$  lamellae with a lower degree of surface order are obtained, as supported by the examination of the overall morphology of thin films.

**Table 5** Overall crystallinity index  $X_c$  (blend) of PEO/PMMA blends and crystallinity index of PEO phase  $X_c$  (PEO) at various compositions and  $T_c$

	$T_c$ (K)	$X_c$ (PEO)	$X_c$ (blend)
Plain PEO10	327	0.81	
	326	0.83	
	325	0.78	
	324	0.80	
	323	0.79	
	322	0.79	
	321	0.78	
	320	0.75	
PEO10/PMMA (90/10)	326	0.81	0.73
	325	0.77	0.69
	324	0.77	0.69
	323	0.77	0.69
	322	0.75	0.68
	321	0.75	0.68
	320	0.74	0.67
	319	0.73	0.66
PEO10/PMMA (80/20)	323	0.82	0.66
	322	0.80	0.64
	321	0.75	0.60
	320	0.73	0.59
	319	0.71	0.57
	318	0.72	0.58
	317	0.69	0.55
	316	0.66	0.53
315	0.66	0.53	
PEO10/PMMA (70/30)	322	0.71	0.49
	321	0.72	0.51
	320	0.72	0.51
	319	0.69	0.48
	318	0.70	0.49
	317	0.67	0.47
	316	0.70	0.49
	315	0.69	0.48
	314	0.69	0.48
	313	0.61	0.43
	312	0.65	0.46
	311	0.65	0.46
PEO10/PMMA (60/40)	320	0.70	0.42
	319	0.66	0.40
	318	0.65	0.39
	317	0.64	0.38
	316	0.69	0.38
	315	0.65	0.39
	314	0.61	0.36
	313	0.62	0.37
	312	0.64	0.38
	311	0.65	0.39

*Temperature dependence of G and  $K_n$*

The influence of the uncrystallizable component on the thermodynamic parameters controlling the spherulitic growth rate and the overall crystallization rate of PEO in the blends has been analysed on the basis of the Turnbull-Fischer equation<sup>14,18</sup>:

$$G = v_2 G_0 \exp[-\Delta F^*/kT_c] \exp[-\Delta\Phi^*/RT_c] \quad (7)$$

where  $\Delta F^*$  is the activation energy for the transport of crystallizing units across the liquid-solid interface,  $\Delta\Phi^*$  is the free energy required to form a nucleus of critical size,  $k$  is the Boltzman constant and  $G_0$  is a term which at low values of  $\Delta T$  may be assumed constant. The pre-exponential factor is multiplied by the PEO volume fraction  $v_2$ , because the rate of nucleation is proportional to the concentration of crystallizable units.

For a polymer-diluent system,  $\Delta\Phi^*$ , according to Boon

and Azcue<sup>15</sup> can be expressed as:

$$\Delta\Phi_{dil}^* = \frac{4b_0\sigma_n\sigma_e T_m}{\Delta H_{2\mu} T} - \frac{2\sigma_e k T_c}{b\Delta T} \ln v_2 \quad (8)$$

where  $\sigma_n$  and  $\sigma_e$  are the interfacial free energies for unit area parallel and perpendicular respectively to the molecular chain axis;  $b_0$  is the distance between two adjacent fold planes;  $\Delta H_{2\mu}$  is the enthalpy of fusion per unit volume of the crystalline component and  $T_m$  its equilibrium melting point. The term containing  $\ln v_2$  in (8) results from entropic contributions to  $\Delta\Phi_{dil}^*$  and is related to the probability of selecting the required number of crystalline polymer sequences in the blends.

The transport term  $\Delta F^*$  may be calculated by means of the Williams, Landel and Ferry relation<sup>16</sup>:

$$\Delta F^* = \frac{C_1 T_c}{C_2 + T_c - T_g} \quad (9)$$

where  $C_1$  and  $C_2$  are constants (generally assumed as 4120 cal mol<sup>-1</sup> and 51.6 K respectively) and  $T_g$  is the glass transition temperature whose value has been calculated for the various blends according to the Fox equation:

$$\frac{1}{T_g} = \frac{W_2}{T_{g2}} + \frac{W_1}{T_{g1}} \quad (10)$$

where  $W_2$  and  $W_1$  are the weight fractions of PEO and PMMA in the blends,  $T_{g2}$  and  $T_{g1}$  the glass transition temperatures of pure components<sup>17</sup>. It has been found in fact that PEO/PMMA blends show a unique  $T_g$  whose value is intermediate between those of pure components and increases with increasing PMMA content<sup>1</sup>. The experimental values of  $T_g$  agree very well with those calculated by the Fox equation, at least for low PEO concentrations where it was possible for us to perform the experiments.

If we assume<sup>8</sup> that  $\sigma_n = 0.1 b_0 \Delta H$ , taking into account relations (8) and (9), the following expression may be written:

$$\begin{aligned} f(G) &= \log G - \log v_2 + \frac{4120}{2.3R(51.6 + T_c - T_g)} - \frac{0.2T_m \log v_2}{\Delta T} \\ &= \log G_0 - \left( \frac{0.4b_0^2\sigma_e}{2.3k} \right) \frac{T_m}{T_c \Delta T} \end{aligned} \quad (11)$$

according to regime I crystallization kinetics.

Analogously, for the overall crystallization rate it is possible to write:

$$\begin{aligned} f(K_n) &= \frac{1}{n} \log K_n - \log v_2 + \frac{4120}{2.3R(51.6 + T_c - T_g)} - \frac{0.2T_m \log v_2}{\Delta T} \\ &= \log A_0 - \left( \frac{0.4b_0^2\sigma_e}{2.3k} \right) \frac{T_m}{T_c \Delta T} \end{aligned} \quad (12)$$

By plotting the quantity  $f(G)$  or  $f(K_n)$  against  $T_m/T_c \Delta T$ , straight lines are obtained as shown in Figures 10 and 11 for the various blends. From the slopes of these lines values of the free energy of folding  $\sigma_e$  have been calculated by using<sup>18</sup>  $\Delta H_{2\mu} = 2.1 \times 10^9$  erg cm<sup>-3</sup> and  $b_0 = 4.65 \times 10^{-8}$  cm.



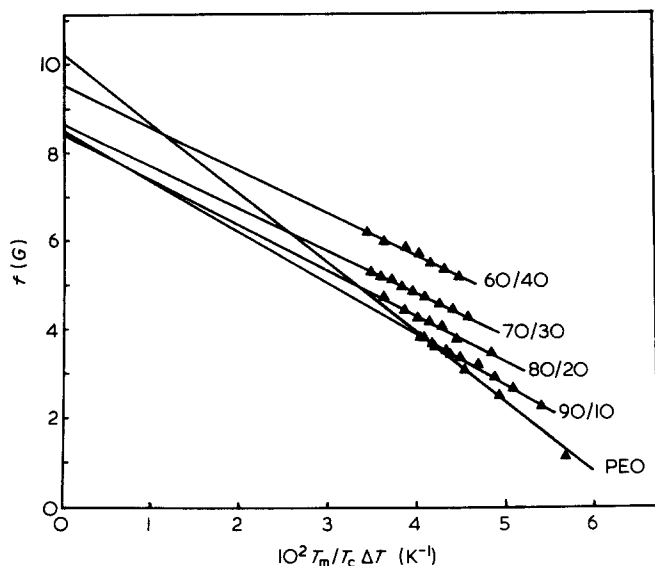


Figure 10 Plots of the quantity  $f(G)$  versus  $T_m/T_c\Delta T$  for PEO10 and its blends with PMMA

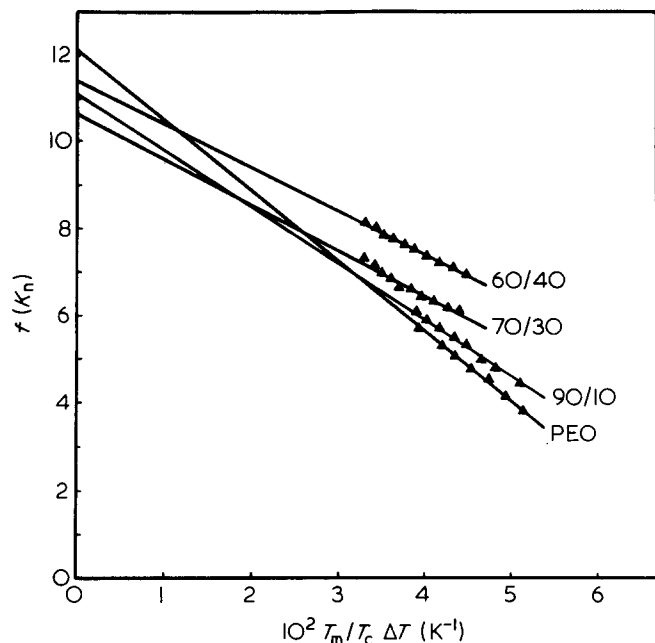


Figure 11 Plots of the quantity  $f(k_n)$  versus  $T_m/T_c\Delta T$  for PEO10 and its blends with PMMA

In Figure 12 the values of  $\sigma_e$  are plotted as function of volume fraction of PEO10 in the blends. As shown  $\sigma_e$  decreases monotonically with increasing PMMA content. For comparison the  $\sigma_e$  of PEO2 and PEO2/PMMA blends is reported in Table 6. It can be seen that in such blends  $\sigma_e$  drops to values that are lower than those of PEO10/PMMA blends.

The above findings are probably related to the fact that during crystallization when PMMA molecules are trapped in interlamellar regions they may easily form entanglements with PEO molecules favouring the formation of larger loops on the surface of PEO lamellar crystals. This process will probably cause the increase of both terms that contribute to  $\sigma_e$ , namely the surface enthalpy and entropy of folding ( $\sigma_e = H_e - TS_e$ ).

The observation that  $\sigma_e$  decreases with increasing PMMA content should be ascribed to the fact that the variation of the entropic term overwhelms that of the enthalpic one.

Finally the larger drop observed in  $\sigma_e$  for PEO2/PMMA blends may be an indication that PMMA molecules interact more with PEO2 molecules and/or that the relative variation of  $S_e$  is larger.

The pre-exponential factors  $G_0$  and  $A_0$ , calculated by extrapolation to the ordinate axis of linear plots in Figures 10 and 11, also depend on the blend composition, showing a parabolic curvature (see Figure 13).

Ong and Price<sup>5</sup> have demonstrated that growth rate data for poly( $\epsilon$ -caprolactone)/poly(vinyl chloride) (PCL/PVC) crystallizable blends could be described by equation (11) only if  $C_2 = 51.6K$  is replaced by  $C_2 = 72K$ . The values of  $f(G)$  calculated for pure PCL and PCL/PVC blends are fitted by the same straight line. For this system then, quantities such as the surface free energy of folding  $\sigma_e$  and  $G_0$  result not to be dependent of composition. Wang and Nishi<sup>6</sup> analysed growth rate data for PVF<sub>2</sub>/PMMA blends by incorporating changes in  $T_g$  and  $T_m$  into a rate theory developed by Lauritzen and Hoffman for homopolymers. Changes in viscosity of the melt and in  $T_g$  were assumed to be responsible for the

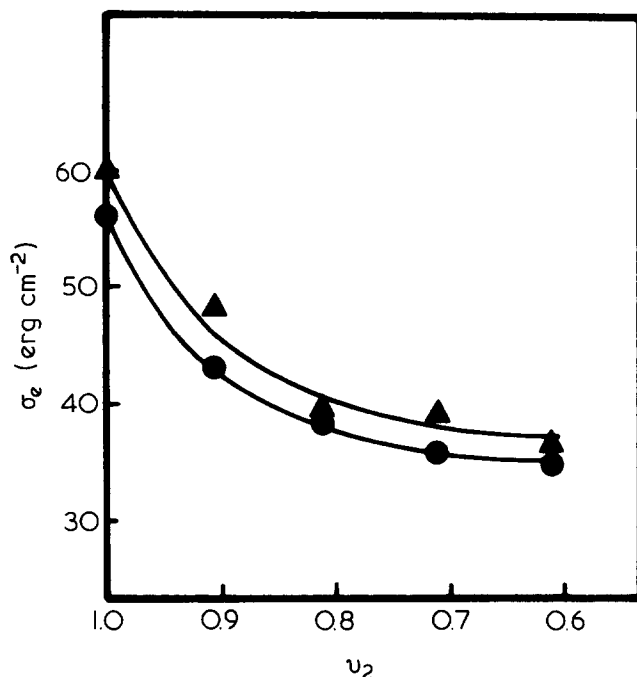


Figure 12 plots of  $\sigma_e$  versus the volume fraction of PEO10 ( $\Delta$ , from  $k_n$  data;  $\bullet$ , from  $G$  data) in blends with PMMA

Table 6 Glass transition temperatures ( $T_g$ ) and free energy of folding of PEO crystals for various blend compositions

PEO/PMMA (w/w)	$T_g$ (K) <sup>a</sup>	$\sigma_e$ (erg cm <sup>-2</sup> ) <sup>b</sup>	$\sigma_e$ (erg cm <sup>-2</sup> ) <sup>c</sup>	$\sigma_e$ (erg cm <sup>-2</sup> ) <sup>d</sup>
100/0	213.2	58	60	57
90/10	223.2	43	48	26
80/20	234.1	38	39	27
70/30	246.2	36	39	22
60/40	259.6	36	37	

<sup>a</sup> From Fox equation taking  $T_g = 385K$  for PMMA

<sup>b</sup> From spherulite growth rate data

<sup>c</sup> From overall crystallization data

<sup>d</sup> From spherulite growth rate of PEO2/PMMA blends (ref. 1)

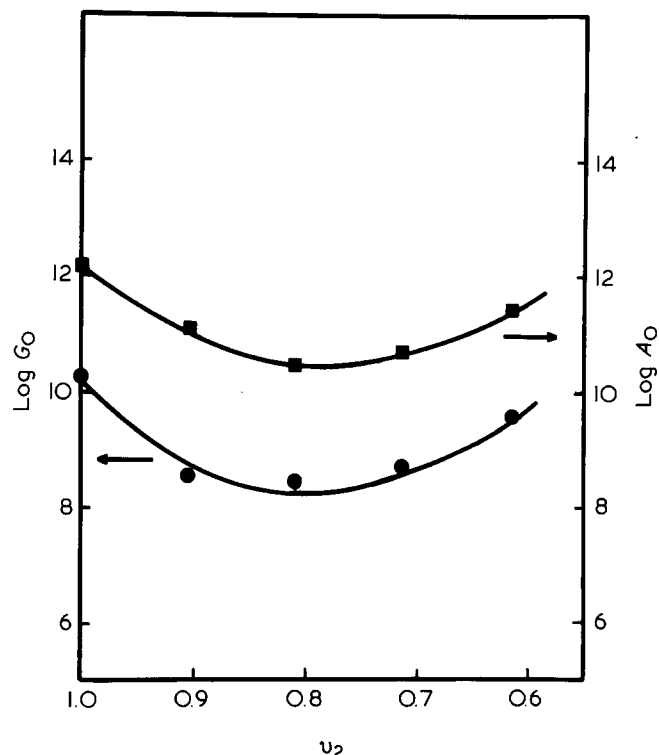


Figure 13 Plots of  $\log G_0$  and  $\log A_0$  versus the volume fraction of PEO10 in blends with PMMA

observed composition dependence. From this analysis it emerges that  $\sigma_e$  is almost independent of composition while the pre-exponential factor  $G_0$  falls rapidly with decrease of  $v_2$ .

#### ACKNOWLEDGEMENT

This work was partly supported by a grant of 'Progetto Finalizzato Chimica Fine' of Italian CNR.

#### REFERENCES

- 1 Martuscelli, E. and Demma, G. B. in 'Polymer Blends: Processing, Morphology and Properties' (Eds. Martuscelli, Kryszewski and Palumbo), Plenum Press, New York, 1980; Martuscelli, E. and Pracella, M. paper in preparation
- 2 Martuscelli, E., Demma, G. B., Rossi, E. and Segre, A. L. *Polymer* 1983, **24** (Commun), 266
- 3 Sanchez, I. C. in 'Polymer Blends' (Eds. Paul and Newman), Academic Press, New York, 1978
- 4 Martuscelli, E., Canetti, M., Vicini, L. and Seves, A. *Polymer* 1982, **23**, 331
- 5 Ong, C. J. and Price, F. P. *J. Polym. Sci. Polym. Symp.* 1978, **63**, 45
- 6 Wang, T. T. and Nishi, T. *Macromolecules* 1977, **10**, 421
- 7 Mandelkern, L. 'Crystallization in Polymers', McGraw-Hill, New York, 1964
- 8 Hoffmann, J. D. *SPE Trans.* 1964, **4**, 315; Hoffman, J. D., Davis, G. T. and Lauritzen, J. I. in 'Treatise on Solid State Chemistry' (Ed. Hannay), Vol. III, Ch. 7, Plenum Press, New York, 1976
- 9 Sanchez, I. C. and Eby, R. K. *Macromolecules* 1975, **8**, 639; Sanchez, I. C. *J. Polym. Sci. Polym. Symp.* 1977, **59**, 109
- 10 Scott, R. L. *Chem. Phys.* 1949, **17**, 279
- 11 Nishi, T. and Wang, T. T. *Macromolecules* 1975, **8**, 909
- 12 Imken, R. L., Paul, D. R. and Barlow, J. W. *Polym. Eng. Sci.* 1976, **16**, 593; Kwei, T. K., Patterson, G. D. and Wang, T. T. *Macromolecules* 1976, **9**, 780
- 13 Bailey, F. E. and Koleske, J. W. in 'Polyethylene Oxide', Academic Press, New York, 1976, p. 142; Brandrup, J. and Immergut, E. H. 'Polymer Handbook', Interscience, New York, 1975
- 14 Turnbull, D. and Fischer, J. C. *J. Chem. Phys.* 1949, **17**, 71
- 15 Boon, J. and Azcue, J. M. *J. Polym. Sci. A-2* 1968, **6**, 885
- 16 Williams, M. L., Landel, R. F. and Ferry, J. D. *J. Am. Chem. Soc.* 1955, **77**, 3701
- 17 Fox, T. G. *Bull. Am. Phys. Soc.* 1956, **2**, 123
- 18 Vidotto, G., Levy, D. L. and Kovacs, A. J. *Kolloid Z.Z. Polym.* 1969, **230**, 289